Structural and dynamical properties of $Mg_{65}Cu_{25}Y_{10}$ metallic glasses studied by in situ high energy x-ray diffraction and time resolved x-ray photon correlation spectroscopy

B. Ruta[1*], V.M. Giordano[2], L. Erra[1], C. Liu[3] and E. Pineda[3]

[1] *European Synchrotron Radiation Facility, BP220, F-38043 Grenoble, France.*
[2] *ILM, Université Claude Bernard Lyon 1 and CNRS, 69622, Villeurbanne, France.*
[3] *Departament Física i Enginyeria Nuclear, ESAB, UPC-BarcelonaTech, Castelldefels, Spain.*

*ruta@esrf.fr

Abstract

We present a temperature investigation of the structural and dynamical evolution of rapidly quenched metallic glasses of $Mg_{65}Cu_{25}Y_{10}$ at the atomic length scale by means of in situ high energy x-ray diffraction and time resolved x-ray photon correlation spectroscopy. We find a flattening of the temperature evolution of the position of the first sharp diffraction peak on approaching the glass transition temperature from the glassy state, which reflects into a surprising slowing down of the relaxation dynamics of even one order of magnitude with increasing temperature. The comparison between structural and dynamical properties strengthens the idea of a stress-induced, rather than pure diffusive, atomic motion in metallic glasses.

Keywords: metallic glasses; structural relaxation; atomic dynamics; internal stresses

1. Introduction

Discovered in the 60s, metallic glasses (MGs) are relatively new materials characterized by a disordered structure which results in a macroscopic behavior that strongly differs from that of the polycrystalline state, and which leads to unique and excellent mechanical properties: a very high tensile strength, a high elasticity and a very good corrosion resistance [1-3].
Above their glass transition temperature, T_g, MGs can be easily deformed without crystallizing in very precise complex shapes, leading to the possibility of using them in a vast range of both commercial and industry applications [1-3]. However, their wide usage is still limited by the metastable nature of the glassy state. The understanding of the glass formation and the relation between the structure, the atomic motion and the unique properties of these remarkable materials is therefore not only fundamental from a theoretical point of view, but it is clearly unavoidable if one wants to use them for practical applications.
Below T_g, MGs – like all glasses – are in an out of equilibrium state and their dynamical and elastic properties depend on the previous thermal history of the sample and will evolve with time [3-9].

Several works have shown the presence of internal stresses or frozen-in excess free volume in rapidly quenched metallic glasses, which lead to a more liquid-like elastic behavior of the material and lower elastic moduli [10-13].
Quantitative information on the presence of extra free volume and its annihilation process under thermal treatment have been usually obtained from high energy X-ray diffraction studies, by following the evolution of static structure factor S(q) for different thermal paths [14-17]. The internal stresses associated to the extra free volume are most likely the reason of the fast exponential physical aging recently observed in the atomic motion of rapidly quenched metallic glasses [8,18,19].
By combining *in situ* x-ray diffraction (XRD) and time resolved x-ray photon correlation spectroscopy (XPCS) measurements, we present here a thoughtful investigation of the structural and dynamical changes occurring at the atomic length scale upon annealing of a rapidly quenched $Mg_{65}Cu_{25}Y_{10}$ glass. The physical aging occurring at the atomic scale has been already investigated by us as reported in Ref. [8]: here we present additional information aimed to relate the observed dynamics to the structural changes occurring in the material upon following different thermal treatments. The analysis of the XRD spectra reveals a peculiar evolution of the main diffraction peak, which can be related to local structural changes during annealing and gives rise to a surprising huge slowing down of the dynamics upon increasing the temperature close to T_g.

2. Materials and methods

Sample preparation. Metallic glasses of $Mg_{65}Cu_{25}Y_{10}$ were obtained by prealloying Cu-Y ingots with the adequate ratio in an arc-melter furnace under a Ti-gettered argon atmosphere and then alloying with magnesium in an induction furnace. The high temperature melt (T ~1250 K) was then fast-quenched with a cooling rate of ~10^6 K/s by injecting it on a copper spinning wheel in a melt spinner device. The resulting ribbons had a thickness of ~33 μm and a width of ~2 mm.
X-ray Diffraction. Diffraction spectra were measured at the beamline ID11 at the European Synchrotron Radiation Facility (ESRF), in Grenoble, France. A high energy beam with a wavelength, λ=0.27 Å (corresponding to an energy of 46 keV) was selected by using a Si(111) monochromator. This energy was chosen for optimizing the resolution on the first sharp diffraction peak (FSDP, q~2.55 $Å^{-1}$). Additional measurements were taken at higher energy with a monochromatic beam of 76 keV (λ=0.16 Å) to cover a larger scattering angle for structural refinement.
Several ribbons with a total thickness of ~300 μm were used and kept in a resistively heated furnace, providing a temperature stability of 0.1 K. During all experiments, the temperature, T, was changed by keeping a fixed heating or cooling rate of 1 K/min.
The temperature evolution of the structure was continuously followed *in situ* by collecting XRD patterns in transmission mode using a fast readout low noise two-dimensional CCD detector FReLoN 2k16 (2048 pixels×2048 pixels, 50 × 50 μm2 pixel size), placed perpendicular to the incident beam.
X-ray Photon Correlation Spectroscopy. XPCS measurements were carried out at the ID10 beamline at ESRF. A partially coherent x-ray beam was focused by using Be compound refractive lens and 8 keV radiation was selected by a single bounce crystal Si(111) monochromator operating in a horizontal scattering. The spatially coherent part of the x-ray beam was selected by using rollerblade slits opened to 10×10 μm, placed ~0.18 m upstream of the sample. The corresponding incident flux on the sample stage was 1.1×10^{10} photons/s/100 mA.

The sample was placed in the same furnace used for the XRD experiments and the scattered intensity was measured in transmission geometry with a IkonM charge-coupled devices from Andor Technology (1024 × 1024 pixels, 13 × 13 μm pixel size) installed ~70 cm downstream of the sample. XPCS measurements were performed for a unique wave-vector q corresponding to the FSDP of the S(q), thereby probing directly the evolution of the dynamics at the inter-particle distance $2\pi/q \sim 2$ Å.
Series up to 3000 images with an exposure time of 5 s or 7 s per image were collected for each temperature, while between scans, the temperature was changed with a fixed rate of 1 K/min. The data were treated and analyzed following the procedure described elsewhere [20,21].

3. Results and Discussion

Diffraction data collected with incident energy of 76 keV are reported in Fig. 1 (a) after the background subtraction and standard data reduction to absolute units. Specifically, the reduction is performed by subtracting from the measured intensity $I(q)=I_{meas}-tI_{bkg}$ (being t the transmission of the sample), a form factor $f^2(q)$ approximating the electron density, the Compton scattering contribution, C(q) [22], and then normalizing to an average form factor:

$$S(q)-1=\frac{I(q)-\sum_{i=1}^{n} f_i(q)^2-C(q)}{\left[\sum_{i=1}^{n} f_i(q)\right]^2} \quad (1)$$

The resulting static structure factor is shown in Fig. 1 upon heating the sample from 300 K up to 423 K. The S(q) is found to be affected by the temperature ramp only in its FSDP (Fig. 1 (a) and (b)). The only evident change is in the integrated intensity of the FSDP, which decreases with temperature up to 350 K and then slowly increases (Fig. 1 (c)). While the first decrease can be explained by the Debye-Waller factor, the following behavior gives indication that something is changing at the atomic level [23].
In order to seize the subtle shape changes of the FSDP, we have measured it with higher resolution by using a lower incident energy of 43 keV and followed it during a first heating ramp up to 423 K (ramp 1), a cooling ramp to room temperature (ramp 2) and a third heating to 423 K (ramp 3). We have fitted the FSDP choosing as fitting range the one where the intensity is larger than 30% of the maximum, and as modeling function an asymmetric pseudo-Voigt, to account for its asymmetric shape. In this function the full width half maximum (FWHM) changes with q as

$$FWHM=\frac{2\Gamma}{(1+e^{\eta(q-q_0)})} \quad (2)$$

The behavior of the ratio $(q_0/q)^3$ and width change Γ/Γ_0 with respect to their low T value before the first heating, and the asymmetry parameter η are reported in Fig. 2. During ramp 1 (full blue circles) all the parameters change their behavior around 360 K: a flattening of the temperature dependence of $(q_0/q)^3$ takes place, accompanied by a sudden narrowing of the FSDP and a more pronounced decrease of its asymmetry. These features could be associated to local rearrangements in the structure and indeed correspond also to a loss of enthalpy in heat capacity measurements, due to the annealing produced by the very slow heating rate with respect to the cooling rate used to produce the glass [13]. On increasing T, $(q_0/q)^3$ slightly further increases up to

about 400 K where it flattens again. It is worth underlying that the narrowing of the FSDP can explain the observed FSDP intensity increase in this range of temperatures.
Upon cooling during ramp 2 (empty red squares), $(q_0/q)^3$ decreases always being lower than during heating, while width and asymmetry are almost constant to their high temperature values. Ramp 3 (full black squares) starts with a position of the FSDP larger than the one of the as-quenched glass. With temperature, the ratio $(q_0/q)^3$ increases again until joining with continuity the one measured during cooling. Width and asymmetry are almost constant and compatible with values from the cooling ramp, suggesting an isostructure configuration during ramp 2 and 3 due to the equivalence between the heating and the cooling rate. Unfortunately due to technical problems part of the data acquired during the first cooling rate have been lost, without however affecting the presented results.
As previously discussed, rapidly quenched metallic glasses keep excess free volume or internal stresses which can be released with the first annealing [10-17].
This phenomenology is due to the intrinsic kinetic nature of the glass transition, and the consequent dependence of T_g on the cooling rate [4,24]. Assuming the atomic environments does not suffer important changes during the annealing, the position of the FSDP can be related to the relative volume change in the material as $V/V_0=(q_0/q)^3$ [14-17]. However, recently, it has been shown that for densely packed metallic glasses this interpretation is not unambiguous and other parameters, such as the FSDP intensity and width can give a clearer indication of the occurrence of structural changes [23].
Overall our results give indication that the glass structure subtly changes with the first annealing, toward a more stable configuration which is kept for successive thermal treatments: the ratio $(q_0/q)^3$ after the first thermal cycle is reduced and then it follows the reversible temperature dependence associated to the heating/cooling rate used during the experiment (Fig. 2 (a)). This process is likely due to stress release or extra volume annihilation, and indeed the $(q_0/q)^3$ behavior suggests a shrinkage of the volume. Differently, the narrowing and symmetrization of the FSDP could be associated to an overall reduction of disorder due to the changes of the most unstable local atomic arrangements. Indeed it is well known that the main irreversible phenomena related to differences in cooling rates are usually observed in the glass transition region, close to T_g.
The changes in the parameters reported in Fig. 2 are remarkably small. In order to confirm that our results are model-independent, we have checked that consistent results can be obtained with another fitting function, specifically a double-pseudoVoigt function. High energy data have also been treated with a Reverse Montecarlo Simulation to have some insight on the structural changes. The weak temperature changes reported in Fig. 2 translates into almost negligible structural changes. We find that the Y atoms are the only ones really involved during the first thermal treatment, their spatial and angular distribution functions being better defined after annealing.
What is intriguing is that the observed weak structural features can reflect into dramatic dynamical changes. Indeed it is well known that structural as well as thermodynamic quantities, like the density or the enthalpy, show only relatively weak temperature dependence in glass formers. Differently, many dynamical quantities, like the viscosity, can significantly vary with temperature. This is the case for instance in the supercooled liquid phase where the static structure factor changes very little while the viscosity or the structural relaxation time, τ, increase many orders of magnitude on approaching T_g [25].

Direct information on the atomic dynamics related to the observed structural rearrangements can be achieved only thanks to the unique properties of XPCS [8,18,19,26,27].

The acquired time-resolved series of scattering intensities were analysed to determine standard intensity time-autocorrelation function $g_2(q,t)$ [28]. This quantity is related to the intermediate scattering function, $f(q,t)$, through the Siegert relation $g_2(q,t)=1+B(q)|f(q,t)|^2$ [28], where $B(q)$ is a setup-dependent parameter. The $f(q,t)$ corresponds to the dynamic structure factor normalized to the $S(q)$ and gives therefore information on the dynamics on a spatial length scale defined by $2\pi/q$. In glass formers, $f(q,t)$ is usually described by the empirical Kohlrausch-Williams-Watt (KWW) function $f(q,t)=f_q\exp(-t/\tau)^{\beta}$ [25], where τ is the characteristic relaxation time, β the shape parameter, and f_q is the nonergodicity plateau before the final decay associated to structural relaxation [29,30].

In order to compare dynamic and structural properties, we performed two ramps in temperature, first heating the as-quenched sample up to 420 K (ramp 1) and then cooling it down again, always with a fixed rate of 1 K/min (ramp 2). The difference with respect to the XRD data is that here the dynamics has been measured by performing different isothermal steps at each temperature, while the XRD data have been acquired while continuously changing T. As discussed later, the different thermal protocol corresponds to a shift of T_g to lower values due to the lower average heating rate.

Figure 3 shows a selection of $g_2(t)$ measured with XPCS during ramp 1. The data are reported together with the best fitting line obtained by using the KWW model. The corresponding structural relaxation times are shown in panel (d) together with equilibrium viscosity data rescaled here in structural relaxation units [31,8]. Three different dynamical ranges are clearly observed: i) on increasing T up to 398 K, the decay of the $g_2(t)$ clearly shifts toward shorter time, indicating that the relaxation time is decreasing and that the dynamics is becoming faster due to thermal motion; ii) for T between 398 K and 408 K the dynamics surprisingly slows down (τ increases); iii) for $T \geq 408$ K the system enters the supercooled liquid phase and the dynamics becomes faster again with T. A smaller increase of τ with temperature is also observed slightly above 360 K in the first dynamical range, in the very same temperature range where a small flatten in the $(q_0/q)^3$ ratio is observed (see Fig. 2) and a loss of enthalpy has been reported [13].

The unexpected step-like behavior of τ below the glass transition temperature is accompanied by a decreasing of the shape exponent β from a constant value of 1.5 in the glass, to $\beta=0.88$ in the supercooled liquid phase. As discussed in Ref. [8] values of $\beta<1$ are typical of glass formers and are often associated to the existence of dynamical heterogeneities, thus of regions of atoms characterized by different relaxation times with respect to the neighboring regions [32]. Differently, shape exponents larger than one are often the hallmark of out of equilibrium dynamics in complex jammed soft materials and are usually associated to ballistic rather diffusive motion due to internal stresses stored in the system in the out of equilibrium state [33,34].

Interestingly the observed slowing down of the dynamics and the decrease in β take place in the same temperature range where the system rearrange its structure and releases the additional stresses related to the fast quenching (see the change of the shape of the FSDP at about 400 K shown in Fig. 2). Thus the structural relaxation observed with XRD appears to be strictly related to a transition from an internal-stress dominated dynamics to a diffusive dynamics in the supercooled liquid phase.

The link between structural and dynamical properties is better highlighted in Fig. 4 where we directly compare the temperature dependence of the ratio $(q_0/q)^3$ measured with XRD, with the variation of relaxation rate γ/γ_0, being $\gamma=1/\tau$. The data are here rescaled as a function of T/T_g, with T_g=410 K for the XRD data, and T_g=405 K for the XPCS. These two different values take into account the different thermal protocols employed during the measurements and have been estimated by differential scanning calorimetric (DSC) measurements in the following way: we have first measured the DSC profile of both an as-quenched sample and a previously annealed one at low T for different cooling rates (5 K/min,10 K/min, and 20 K/min), and then we have estimated the corresponding T_g values at the rate of the XPCS experiment through the well-known relation between T_g and temperature rate proposed by Moynihan in 1974 [8,35]. Figure 4 clearly shows that the dynamics completely mimics the structural changes. In both cases the rapidly quenched sample starts to deviate from the low temperature behavior at about 260 K (~0.65 T/T_g), where the system starts to release the stresses introduced during the quenching. Here, a flattening of the $(q_0/q)^3$ (T) dependence corresponds to a decrease in the relaxation rate (and thus an increase in τ, see Fig. 3 **d**). This effect is even more evident close to the glass transition temperature, at ~385 K (~0.95 T/T_g), where γ decreases of almost one order of magnitude before further increasing in the supercooled liquid phase. A change of the temperature dependence of $(q_0/q)^3$ in the liquid phase is not observed here, being likely located at higher temperatures. Indeed, XPCS measurements on as-quenched samples continuously heated up at 1 K/min show that the system joins the supercooled liquid dynamics at ~417 K [8], in agreement with the XRD data.
The comparison between the dynamical and structural results supports the interpretation of the shape changes of the FSDP as due to internal stresses release. It is worth underlying here that a difference of 6 order of magnitude in cooling rates between the fast cooling rate (~10^6 K/s) used to produce the glass, and the slow cooling rate (1 K/min) applied in this experiment, gives rise to a residual reduction of $(q_0/q)^3$, and thus indirectly of the volume, as small as 0.5%, while it corresponds to a slowing down of the atomic motion of more than one order of magnitude.

4. Conclusions

We have investigated the structural and dynamical changes occurring at the atomic length scale in a rapidly quenched $Mg_{65}Cu_{25}Y_{10}$ metallic glass, by combining high energy *in situ* XRD and time resolved XPCS measurements.
The position, width, and intensity of the first peak in the XRD patterns exhibit a nearly linear behavior on increasing the temperature up to around 360 K where a first flattening of the temperature dependence of the ratio $(q_0/q)^3$ takes place, accompanied by a sudden narrowing of the FSDP and a more pronounced decrease of its asymmetry. On increasing T, $(q_0/q)^3$ slightly increases again and then becomes constant at about 400 K. Similar results have been previously reported in the case of several metallic glasses and have been associated to the annihilation of the free volume or internal stresses introduced in the sample during the fast quenching used to produce the material [14-17]. However such an association is still debated, and the direct relation between $(q_0/q)^3$ and the volume change has been shown to be ambiguous [23].
The corresponding atomic dynamics has been measured with XPCS by monitoring the temperature dependence of the intermediate scattering function under similar thermal treatments. We find that the observed tiny structural changes (less than 1%) reflect

into a complex behavior of the atomic dynamics. In particular we find that these changes take place at ~0.95 T/T_g where the corresponding dynamics surprisingly slows down of an order of magnitude with increasing T. Similar structural and dynamical behaviors have been recently reported in Vit.1 [36], and in the sub-T_g enthalpy relaxation in CuZrAl metallic glasses [37]. In both cases these behaviors have been related to strong to fragile liquid-liquid phase transitions above T_g.
In our case, the increase in the characteristic time for structural rearrangements is furthermore accompanied by a decrease in the shape exponent from a compressed value (>1) to the usual stretched (<1) value of supercooled liquids. As discussed in Refs. [33,34], shape exponents larger than one are usually found in complex soft materials and are associated to a ballistic rather than diffusive dynamics due to internal stresses introduced in the material when it falls out of equilibrium. Our analysis suggests the presence of a very similar physical mechanism responsible for the dynamics of rapidly quenched metallic glasses.

Acknowledgment
We gratefully thank F. Nazzani and all the staff of the beamline ID10 and ID11 at the ESRF for the support during the measurements, and H. Vitoux for the technical support. M. Di Michiel is acknowledged for useful discussions. E. Pineda and C. Liu acknowledge financial support from CICYT Grant MAT2010-14907 and Generalitat de Catalunya Grants 2009SGR1251 and 2012FI-DGR.

References

[1] *Bulk Metallic Glasses: An overview*. M. Miller and P. Liaw, Springer, 2007.

[2] W. H. Wang, Prog. Mater. Sci. 57 (2012) 487.

[3] C. J. Byrne and M. Eldrup, Science 321 (2008) 502.

[4] P. G. Debenedetti and F.H. Stillinger, Nature 410 (2001) 259

[5] P. Wen, G.P. Johari, R.J. Wang and W.H. Wang, Phys. Rev. B 73 (2006) 224203

[6] R. Busch, R. Bakke and W.L. Johnson, Acta Mater. 46 (1988) 4725.

[7] V.A. Khonik, Yu. P. Mitrofanov, S. A. Lyakhov, A. N. Vasiliev, S. V. Khonik and D. A. Khoviv, Phys. Rev. B 79 (2009) 132204.

[8] B. Ruta, Y. Chushkin, G. Monaco, L. Cipelletti, E. Pineda, P. Bruna, V. M. Giordano, and M. Gonzalez-Silveira, Phys. Rev. Lett., 109 (2012) 165701.

[9] J. Hachenberg, D. Bedorf, K. Samwer, R. Richert, A. Kahl, M.D. Demetriou and W.L. Johnson, Appl. Phys. Lett. 92 (2008) 131911.

[10] M. H. Cohen and D. Turnbull, J. Chem. Phys., 31 (1959) 1164.

[11] A. I.Taub and F. Spaepen, Acta Metall. 28 (1980) 1781.

[12] Z. Evenson and R. Busch, Acta Mater. 59 (2011) 4404.

[13] E. Pineda, P. Bruna, B. Ruta, M. Gonzalez-Silveira and D. Crespo, Acta Mater. 61 (2013) 3002.

[14] A. R. Yavari et al., Acta Mat., 53 (2005) 1611.
[15] J. Bednarcik, S. Michalik, M. Sikorski, C. Curfs, X.D. Wang, J.Z. Jiang and H. Franz, J. Phys.: Condens. Matter 23 (2011) 254204.
[16] N. Zheng, G. Wang, L.C. Zhang, M. Calin, M. Stoica, G. Vaughan, N. Mattern and J. Eckert J. Mater. Res., 25 (2010) 2271.
[17] E. Pineda, I. Hidalgo, P. Bruna, T. Pradell, A. Labrador and D. Crespo, J. Alloy and Compd. 483 (2009) 578.
[18] B. Ruta, G. Baldi, G. Monaco, and Y. Chushkin, J. Chem. Phys. 138 (2013) 054508.
[19] B. Ruta, Y. Chushkin, G. Monaco, L. Cipelletti, V. M. Giordano, E. Pineda and P. Bruna, AIP. Conf. Proc. 1518 (2013) 181.
[20] L. Cipelletti, and D.A. Weitz, Rev. Sci. Instrum. 70 (1999) 3214.
[21] Y. Chushkin, C. Coronna and A.Madsen, J.Appl.Cryst. 45 (2012) 807.
[22] C. J.Benmore "A Review of High-Energy X-Ray Diffraction from Glasses and Liquids" ISRN Material Science, Volume 2012, Article ID 852905.
[23] N. Mattern, M. Stoica, G. Vaughan and J. Eckert, Acta Mater. 60 (2012) 517.
[24] I.M. Hodge, J. Non-Cryst. Sol. 169 (1994) 211.
[25] C. A. Angell, K.L. Ngai, G.B. McKenna, P.F. McMillan and S.W. Martin, J. Appl. Phys. 88 (2000) 3113.
[26] M. Leitner, Bogdan Sepiol, L.M. Stadler, B. Pfau and G. Vogl, Nature Mat. 8 (2009) 717.
[27] M. Leitner, B. Sepiol, L. M. Stadler, and B. Pfau, Phys. Rev. B 86 (2012) 064202.
[28] G Grübel, A Madsen, A Robert, Soft-Matter Characterization, "18. X-ray Photon Correlation Spectroscopy", R. Borsali and R. Pecora, Springer (2008).
[29] B. Ruta, G. Monaco, V. M. Giordano, F. Scarponi, D. Fioretto, G. Ruocco, K. S. Andrikopoulos and S. N. Yannopoulos, J. Phys. Chem. B, 115 (2011) 14052.
[30] B. Ruta, G. Baldi, F. Scarponi, D. Fioretto, V. M. Giordano and G. Monaco. J. Chem. Phys. 137 (2012) 214502.
[31] R. Busch, W. Liu and W.L. Johnson,J. Appl. Phys. 83 (1998) 4134.
[32] M. D. Ediger and P. Harrowell, J. Chem. Phys. 137 (2012) 080901.
[33] L. Cipelletti, L. Ramos, S. Manley, E. Pitard, D. A. Weitz, E. Pashkovski and M. Johansson, Faraday Discuss. 123 (2003) 237.
[34] J. P. Bouchaud and E. Pitard, Eur. Phys. J. E 6 (2001) 231.
[35] C. T. Moynihan, A. J. Easteal, and J. Wilder, J. Phys. Chem. 78 (1974) 2673.
[36] S. Wei, F. Yang, J. Bednarcik, I. Kaban, O. Shuleshova, A. Meyer and R. Busch, Nature Comm. 4 (2013) 1.
[37] L. Hu, Y. Yue and C. Zhang, App. Phys. Lett. 98 (2011) 081904.

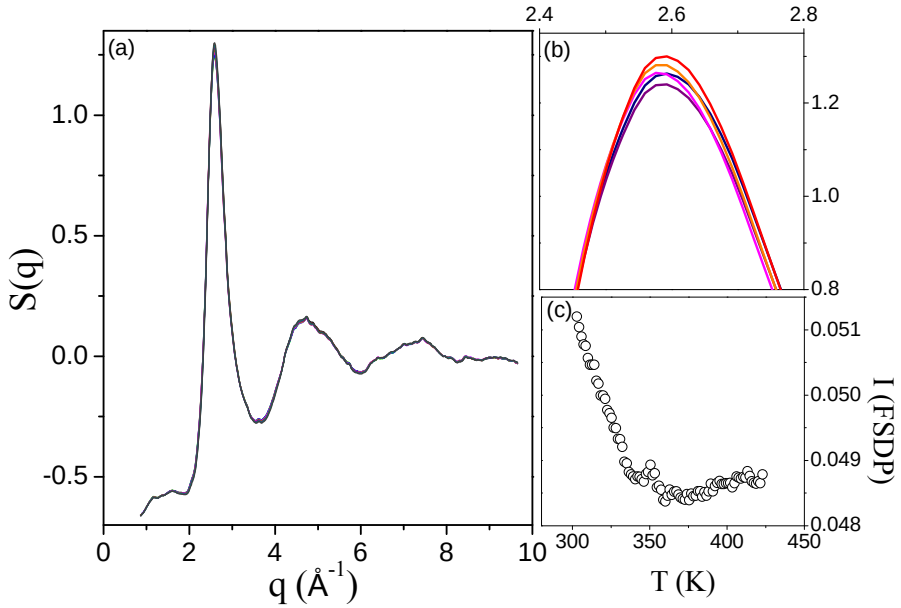

Fig. 1. **a,** S(q) data for sample 2 during heating from 300 K to 423 K, after background subtraction and normalization to absolute units. **b**, zoom of the FSDP showing the subtle changes with increasing T. The curves correspond to 30 K (blue), 332 K (purple), 360 K (magenta), 388 K (orange) and 423 K (red). **c**, Temperature behavior of the integrated intensity of the FSDP.

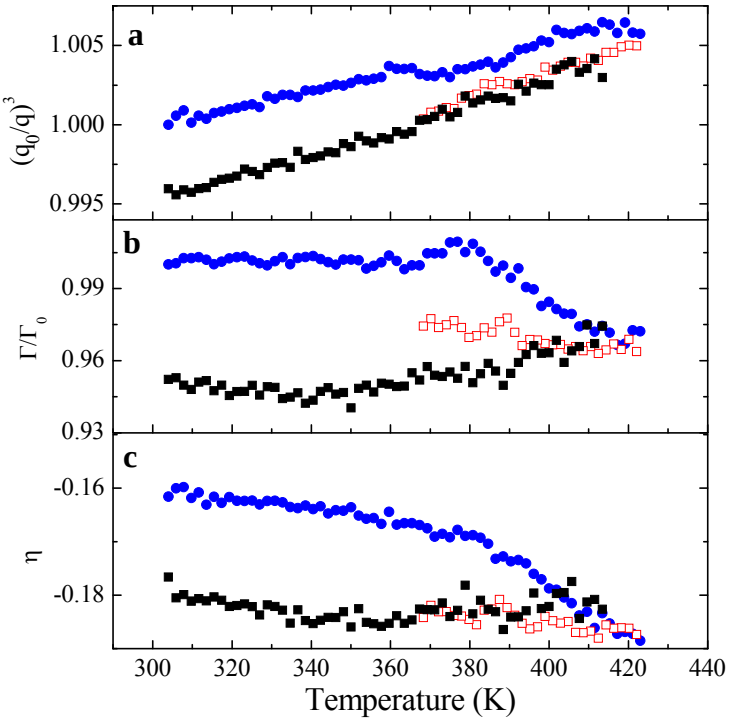

Fig. 2. (color online) **a,** Evolution of the position of the FSDP in sample 1 after annealing to 423 K. The FSDP has been fitted using an asymmetric pseudo-voigt function (see text). The data have been rescaled for the value at 300 K in the as-quenched glass (**a**) during the first annealing (blue circles), cooling (red empty squares) and second heating (black squares). The change in the relative width with

respect to the as-quenched value and the asymmetry parameter describing the FSDP are reported in panels (**b**) and (**c**), respectively. The free volume relaxation is accompanied by an irreversible narrowing of the FSDP and a reduction of its asymmetry.

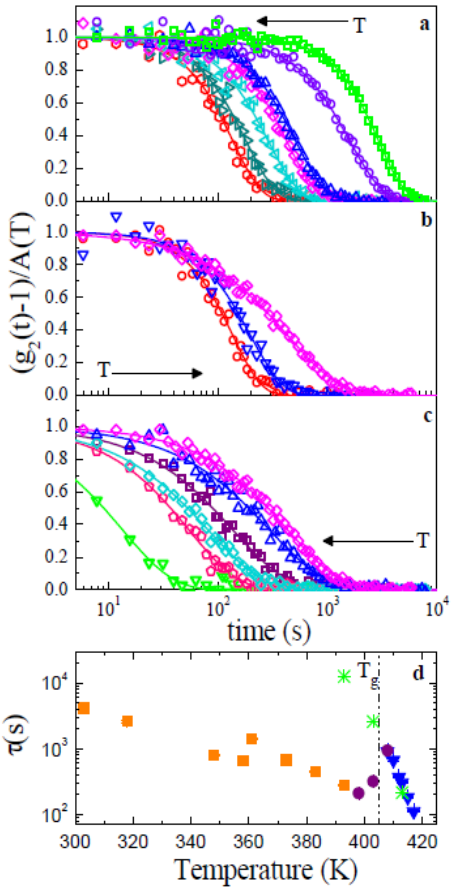

Fig. 3. (color online) Normalized intensity correlation functions measured with XPCS in the as-quenched glass upon ramp 1. The black arrows indicate the evolution under increasing temperature. As explained in the text, three dynamical range are observed: **a**, the dynamics gets faster (τ decreases) on increasing T from 300 K up to 398 K; **b**, a surprising slowdown of the atomic motion (τ increases) takes place between 398K≤ T ≤408 K; **c**, the dynamics gets faster again for T ≥408 K . **d**) Corresponding relaxation times obtained from the analysis of the $g_2(t)$ with a KWW model function (full symbols), together with the macroscopic equilibrium value taken from Refs. [31] (stars). Squares, circles and down triangles corresponds to the data reported in panels **a**, **b**, and **c**, respectively.

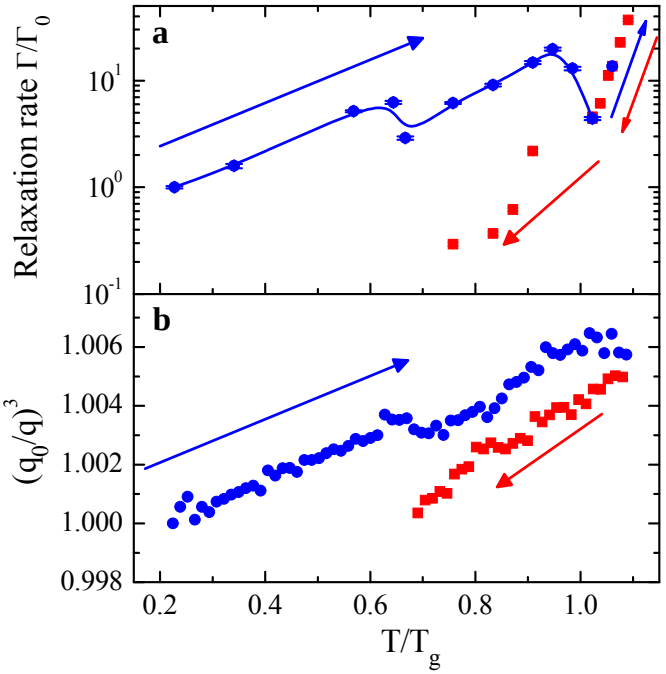

Fig. 4. (color online) Temperature dependence of the relaxation rate (**a**) and of $(q_0/q)^3$ (**b**) obtained from the analysis of atomic dynamics measured with XPCS (**a**) and the evolution of the static structure factor with XRD (**b**). The arrows indicate the temperature changes. Both quantities are rescaled for the corresponding value at low temperature and reported as a function of the temperature rescaled by T_g.